Backbone modified TBA analogues endowed with antiproliferative activity ☆

Veronica Esposito, Annapina Russo, Teresa Amato, Michela Varra, Valentina Vellecco, Mariarosaria Bucci, Giulia Russo, Antonella Virgilio *, Aldo Galeone *

Department of Pharmacy, University of Naples Federico II, Via D. Montesano 49, I-80131 Naples, Italy

ABSTRACT

Background: The thrombin binding aptamer (TBA) is endowed with antiproliferative properties but its potential development is counteracted by the concomitant anticoagulant activity.
Methods: Five oligonucleotides (ODNs) based on TBA sequence (GGTTGGTGTGGTTGG) and containing L-residues or both L-residues and inversion of polarity sites have been investigated by NMR and CD techniques for their ability to form G-quadruplex structures. Furthermore, their anticoagulant (PT assay) and antiproliferative properties (MTT assay), and their resistance in fetal bovine serum have been tested.
Results: CD and NMR data suggest that the investigated ODNs are able to form right- and left-handed G-quadruplex structures. All ODNs do not retain the anticoagulant activity characteristic of TBA but are endowed with a significant antiproliferative activity against two cancerous cell lines. Their resistance in biological environment after six days is variable, depending on the ODN.
Conclusions: A comparison between results and literature data suggests that the antiproliferative activity of the TBA analogues investigated could depends on two factors: a) biological pathways and targets different from those already identified or proposed for other antiproliferative G-quadruplex aptamers, and b) the contribution of the guanine-based degradation products.
General significance: Modified TBA analogues containing L-residues and inversion of polarity sites lose the anticoagulant activity but gain antiproliferative properties against two cancer cell lines. This article is part of a Special Issue entitled "G-quadruplex" Guest Editor: Dr. Concetta Giancola and Dr. Daniela Montesarchio.

© 2016 Published by Elsevier B.V.

1. Introduction

RNA and DNA aptamers can be defined as short synthetic ribo- and deoxyribonucleic acids able to bind, with high affinity and specificity, a broad range of molecular targets as small molecules, proteins and other nucleic acids [1,2]. In general, these remarkable ligands result from several cycles of an in vitro selection strategy called SELEX (Systematic Evolution of Ligands by EXponential enrichment) and, owing to their outstanding properties, are quickly becoming well-developed tools for numerous applications in research, diagnosis and therapy [2]. Under certain conditions and in aqueous solution, aptamers are able to fold in stable three-dimensional structures conferring on them the ability to bind their cognate ligands. Several DNA/RNA secondary motifs, as e.g. hairpins, pseudoknots, loops, can belong and

contribute to the structural stability of these ligands, this property being a key feature for the aptamer development and application. A significant number of aptamer sequences, discovered by chance or picked by in vitro selection techniques, adopt K^+ ion dependent G-quadruplex structures, which are among the most stable and common nucleic acids conformations identified by this approach [3,4].

Apart from G-quadruplex aptamers with a role in analytics, also G-quadruplex ligands of therapeutic interest have been identified [3,4]. In this frame, the antiproliferative and anticancer G-quadruplex aptamers have assumed a notable importance, particularly taking into account their degree of development in clinical investigations [5,6]. A noteworthy example is the aptamer $(GGGC)_4$ (T40214) forming a parallel G-quadruplex targeting the signal transducer and activator of transcription 3 protein (Stat3) [7]. Recently, two G-quadruplex DNA aptamers have been selected against epidermal growth factor receptor (EGFR)-transfected A549 cells and their antiproliferative properties have been tested [8]. In 2010 Bates et al. suggested that the cancer-selective antiproliferative activity may be a general feature of certain G-rich oligodeoxynucleotides (ODNs) and is associated with the formation of G-quadruplex structures [9]. In a previous investigation,

Bates et al. described the physical properties and biological activity of a group of 12 G-quadruplex forming ODNs [8]. Among these, KS-B ($G_2T_2G_2TGTG_2T_2G_2$, corresponding to TBA: thrombin binding aptamer) and GRO29A ($T_3(G_2T)TG(TG_2)_4$) showed the best two antiproliferative activities against HeLa cervical carcinoma cells. Afterwards, GRO29A was proven to be active also without the first three thymidines (AGRO100 or AS1411: $(G_2T)_4TG(TG_2)_4$) [11,12] and, then, the following detailed investigations were carried out on this sequence [5,13]. Aptamer AS1411 has showed promising antineoplastic effects and several studies have indicated that the target of aptamer AS1411 is the surface nucleolin [11,12,14], a multifunctional protein present in the nucleolus and nucleus of most cells, as well as in the cytoplasm and on the surface for some cells, including cancer cells and angiogenic endothelial cells. These data suggest that the biological properties of AS1411 may be attributed to interference with the multitude of nucleolin-mediated cell processes. In contrast with the large quantity of biological and pre-clinical studies, only a few investigations have been devoted to the structural features of the G-quadruplex conformation adopted by AS1411, probably due to the high degree of polymorphism showed by this aptamer [15]. Interestingly, NMR and X-ray investigations on a sequence derived from that of AS1411, namely $T(G_2T)_4TG(TG_2)_3TGT_2$, showed that it is able to form an unusual left-handed G-quadruplex structure [16].

Contrarily to the polymorphism of AS1411, TBA folds in a well defined antiparallel G-quadruplex structure characterized by two stacked G-tetrads connected through three loops [17,18]. Unfortunately, the development of TBA as an antiproliferative agent has been severely counteracted by its concomitant anticoagulant activity and low thermal stability in physiological condition.

In view of the previous discussion, in developing TBA analogues potentially endowed with antiproliferative properties, these main points should be taken into account: 1) the propensity of the sequence to form a major G-quadruplex structure should be preserved; 2) the modified aptamer should retain no or a negligible anticoagulant activity; 3) the resistance of the aptamer to nucleases should be enhanced.

A recent paper has reported that the site specific replacement of single nucleosides into a loop with a dibenzyl linker is able to switch the activity of TBA from anticoagulant to antiproliferative against He-La cervical carcinoma cells [19]. In previous investigations, we have described the preparation of TBA analogues containing L-residues (whose structures are mirror images of the natural D-residues) or both L-residues and inversion of polarity sites, in an attempt to obtain modified aptamers with better properties [20,21]. Here we report data on some of them (Table 1), concerning both the anticoagulant and the antiproliferative properties on two different cancerous cell lines.

2. Materials and methods

2.1. Oligonucleotides synthesis and purification

Modified ODNs reported in Table 1 were prepared and purified as previously reported [20,21]. Briefly, ODNs were synthesized on a Millipore Cyclone Plus DNA synthesizer using solid phase β-cyanoethyl phosphoramidite chemistry at 15 μmol scale. The synthesis of the 3′–5′ tracts were performed by using normal 3′-phosphoramidites, 5′-dimethoxytrityl-β-L-deoxyguanosine (iBu)-3′-phosphoramidite and 5′-dimethoxytrityl-β-L-deoxythymidine-3′-phosphoramidite, whereas the 5′–3′ tracts were synthesized by using 5′-phosphoramidites. All modified phosphoramidite monomers are commercially available (ChemGenes). For all ODNs an universal support was used.

The oligomers were detached from the support and deprotected by treatment with concentrated aqueous ammonia at 80 °C overnight. The combined filtrates and washings were concentrated under reduced pressure, redissolved in H_2O, analyzed and purified by high-performance liquid chromatography on a Nucleogel SAX column (Macherey-Nagel, 1000-8/46), using buffer A: 20 mM KH_2PO_4/K_2HPO_4 aqueous solution (pH 7.0) containing 20% (v/v) CH_3CN and buffer B: 1 M KCl, 20 mM KH_2PO_4/K_2HPO_4 aqueous solution (pH 7.0) containing 20% (v/v) CH_3CN; a linear gradient from 0 to 100% B for 45 min and flow rate 1 ml/min were used. The fractions of the oligomers were collected and successively desalted by Sep-pak cartridges (C-18). The isolated oligomers proved to be >98% pure by NMR.

2.2. Nuclear magnetic resonance

NMR samples were prepared at a concentration of about 1.5 mM, in 0.6 ml (H_2O/D_2O 9:1 v/v) buffer solution having 10 mM KH_2PO_4/K_2HPO_4, 70 mM KCl and 0.2 mM EDTA (pH 7.0). All the samples were heated for 5–10 min at 80 °C and slowly cooled (10–12 h) to room temperature. The solutions were equilibrated for several weeks at 4 °C. The annealing process was assumed to be complete when ^{1}H NMR spectra were superimposeable on changing time. NMR spectra were recorded with a Varian Unity INOVA 700 MHz spectrometer. 1D proton spectra of the samples in H_2O were recorded using pulsed-field gradient DPFGSE for H_2O suppression [22]. ^{1}H-chemical shifts were referenced relative to external sodium 2,2-dimethyl-2-silapentane-5-sulfonate (DSS).

2.3. Prothrombin time (PT) assay

PT assay on human plasma samples was measured by using Koagulab MJ Coagulation System with a specific kit HemosIL RecombinPlasTin 2G (Instrumentation Laboratory, Milan, Italy). Briefly, this method relies on the high sensitivity of thromboplastin reagent based on recombinant human tissue factors. The addiction of recombiplastin to the plasma, in presence of calcium ions, initiates the activation of extrinsic pathway converting the fibrinogen into fibrin, with a formation of solid gel. The procedure was performed according to the manufacturer's instructions. In our experimental conditions, each ODN or vehicle was incubated with 100 μl of plasma at 37 °C for 15 min after that 200 μl of the kit solution containing recombiplastin was added with consequent activation of extrinsic pathway. In details, 2 μl of the corresponding ODN solution (1 mM in PBS) or vehicle (PBS) was added in the apposite microtube, in order to achieve the final concentration of 20 μM. The PT measurement was produced in triplicate and the average and its standard error values were calculated and expressed as seconds. The basal clotting time was determined by measuring the clotting time in absence of any ODN. Incubation with PBS did not modify the PT measurement.

2.4. Cell cultures and treatments with the ODNs

Human p53 mutated lung cancer Calu-6 (ATCC® HTB-56™) and p53 null colorectal cancer cell lines HCT 116$^{p53 -/-}$ [23] cell lines were cultured in Dulbecco's Modified Eagle's Medium (DMEM), supplemented with 10% fetal bovine serum (FBS) (Euroclone S.p.A), 2 mM L-glutamine and 50 U/ml penicillin-streptomycin, under

Table 1
Sequences investigated and their melting temperatures (T_m).

Name	Sequence[a]	T_m (°C)[b]	G-quadruplex[c]
TBA	5′-G G T T G G T G T G G T T G G-3′	50	right–handed
TBA all–L	5′-g g t t g g t g t g g t t g g-3′	50	left–handed
D13	5′-g g T T g g t g t g g T T g g-3′	52	left–handed
IL4	5′-g g x T T • g g t g t g g x T T • g g-3′	50	left–handed
ID6	5′-g g x T T • g g x TGT • g g x T T • g g-3′	41	left–handed
ULDD	5′-g G T T G g t g t g G T T G g-3′	42	right–handed

[a] D and L residues are indicated in upper and lower case, respectively. Inversion of polarity sites 3′–3′ and 5′–5′ are indicated by a x and a dot, respectively. Loop residues in the original TBA structure are highlighted in red.
[b] See Refs. 20,21.
[c] According to the CD spectra.

humidified atmosphere of 5% CO_2 at 37 °C. Treatments of cells were performed replacing the culture medium with those containing different ODNs at final concentration of 10 μM and 50 μM per well from 24 h to 144 h.

2.5. MTT assay

Calu-6 [24] and HCT 116$^{p53 −/−}$ cells [25] were seeded onto 96-well plates at density of 2 × 104 cells/well and treated with different ODNs at final concentration of 10 μM and 50 μM from 24 h to 144 h. Then, cell viability was determined using the MTT assay as previously reported [26]. A pool of three different sets of experiments each repeated in triplicate were performed. Error bars represent mean ± SEM from n = 3 biological replicates. Statistical comparisons were made as previously shown [27].

2.6. Nuclease stability assay

Nuclease stability of anti-thrombin aptamers was evaluated in 10% fetal bovine serum (FBS) diluted with Dulbecco's Modified Eagle's Medium (DMEM) at 37 °C. Approximately 7 nmol of stock solution of each ODN (~1 O.D.U.) was evaporated to dryness under reduced pressure and then incubated with 250 μl 10% FBS at 37 °C. At 0 and 144 h, 125 μl of samples were collected and stored at −20 °C for at least 20 min. The samples were evaporated to dryness and then 10 μl of gel loading buffer and 10 μl of autoclaved water were added. 10 μl of the mixture was used for polyacrylamide gel electrophoresis (PAGE), which was carried out at room temperature using 20% polyacrylamide gel in 1× TBE buffer (Tris-borate-EDTA). The degradation patterns on the gel were visualized by UV shadowing. The band intensity of the stained gel was quantified by densitometry with ImageJ software.

3. Results and discussion

3.1. Structural insight of the investigated sequences

It is well known that TBA is able to fold in a peculiar monomolecular, antiparallel G-quadruplex structure with a "chair-like" conformation. The core of the G-quadruplex is characterized by two stacked G-tetrads in which *syn* and *anti* guanosines alternate both in each G-tetrads and along the strands. Furthermore, the two G-tetrads are linked to each other by differently sized edge-wise loops: a central loop (sequence TGT) and two lateral loops (sequence TT) (Fig. 1) [17,18].

A convincing amount of studies suggested that the two TT loops represent the most important regions of the aptamer involved in the interaction with the thrombin anion exosite I and, therefore, they are mostly responsible for the anticoagulant activity of TBA [28–30]. On the other hand, the same investigations also suggested a minor role for the TGT loop being able to interact with the heparin binding site of a further thrombin molecule. Hence, similarly to other G-quadruplex aptamers, the structure of TBA is characterized by a central part composed of stacked G-tetrads, mostly accounting for the thermal stability, and by some loops protruding outward and, then, more prone to interact with the target proteins. In the selection of TBA analogues as potential antiproliferative aptamers, we have mainly taken into account three properties: 1) the ability to form G-quadruplex structures; 2) the thermal stability in physiological conditions and 3) the chemical resistance in biological environments. Recently, in an effort to obtain TBA analogues with improved properties, we have prepared and investigated sequences containing L-nucleotides or both L-nucleotides and inversion of polarity sites [20,21]. Among these, ODNs have been chosen showing different composition and strand orientation of loop sequences in the original chair-like structure (Table 1).

Circular dichroism is an important technique, not only to ascertain the occurrence of G-quadruplex structures in solution but also to obtain information regarding the folding topology, particularly in the case of sequences analogues of a parent ODN, for which the formation of a peculiar G-quadruplex has been assessed by other techniques and whose CD profile is known [31]. In Fig. 2 the CD profiles of the ODNs investigated are shown in comparison with that of the natural TBA. Since **TBA all-L** shows the same sequence as TBA but is composed by only L-residues, its CD profile is perfectly specular to that of TBA, as expected. Therefore, **TBA all-L** folds in a left-handed chair-like G-quadruplex structure that is the mirror image of the TBA structure. ODN **D13** is mostly composed by L-residues, apart from thymidines forming the two small lateral loops, namely T3, T4, T12 and T13. Its CD spectrum shows a profile very similar to that of **TBA all-L**, thus suggesting the occurrence of a left-handed chair-like G-quadruplex structure also for this case (Fig. 1). ODN **IL4** shows sequence and base composition analogous to **D13** but, in this case, two 3′–3′ (in between G2–T3 and G11–T12) and two 5′–5′ (in between T4–G5 and T13–G14) inversion of polarity sites have been introduced with the aim to invert the strand direction of the small loops TT, in respect to **D13**. Two further inversion of polarity sites (one 3′–3′ and one 5′–5′ in between G6–T7 and T9–G10, respectively) have been added in the sequence of ODN **ID6** in order to invert also the strand direction of the large loop TGT. Also CD spectra of ODNs **IL4** and **ID6** show profiles similar to that of **TBA all-L**, besides slight differences regarding the band intensities and their wavelengths. Therefore, also for these cases, we proposed left-handed chair-like G-quadruplex structures (Fig. 1). These results should not be considered particularly surprising taking into consideration that, in the cases for which a left-handed G-quadruplex structure has been proposed, (namely, **TBA all-L**, **D13**, **IL4** and **ID6**) all guanosines forming the two-G-tetrad core in the original chair-like conformation are L-residues, thus ruling the handedness of the whole structure.

It should be noted that although **IL4** and **ID6** form both left-handed G-quadruplex structures, the melting temperature of **IL4** is about 9 °C higher than **ID6**. Considering their different structures, this datum should not be considered unexpected. In fact, in the more stable **IL4**, residues in G-tetrads and TGT loop (which are the parts mostly responsible for the thermal stability [32–34]) share the same chirality and are linked through canonical 3′–5′ phosphodiester bonds. On the contrary, in **ID6**, residues in the G-tetrads and TGT loop show opposite chirality and two inversion of polarity sites, thus negatively affecting the structural stability.

Differently from the other ODNs, sequence of **ULDD** is the only one in which four guanosines forming the G-quadruplex stem in TBA are D-residues while the other belong to the L-series. Therefore, in this case, there is not a strong factor ruling the G-quadruplex handedness. In fact, the CD spectrum of **ULDD** (Fig. 2) shows a profile quite different from those of the other TBA analogues and their natural counterpart, being characterized by a negative and a positive band at 245 and 266 nm, respectively. Taking into account a) the resemblance of the CD profile of **ULDD** with that of the tetramolecular G-quadruplex formed by TG$_4$T (Fig. 2), b) the dependence of the CD profile from the type of the G-tetrad stacking [35] and, c) the relationship between glycosidic bond of L-guanosines and strand directionality in G-quadruplex structures previously studied [36], for **ULDD** we proposed the right-handed chair-like G-quadruplex conformation showed in Fig. 1.

In an attempt to obtain more structural information and to confirm the presence of G-quadruplexes for the TBA analogues, we have also recorded ^{1}H NMR spectra. In Fig. 3, the imino and aromatic proton regions are shown. As expected, **TBA all-L** showed a spectrum identical to its enantiomer TBA. In the case of **D13**, the simple appearance of its spectrum and the presence of eight partially overlapped signals in the G-quadruplex diagnostic region between 10.5 and 12.5 ppm (in which the guanosine imino protons involved in H-bonds occur) clearly indicated the formation of a well-defined G-quadruplex structure. More detailed 2D-NMR investigations confirmed a monomolecular
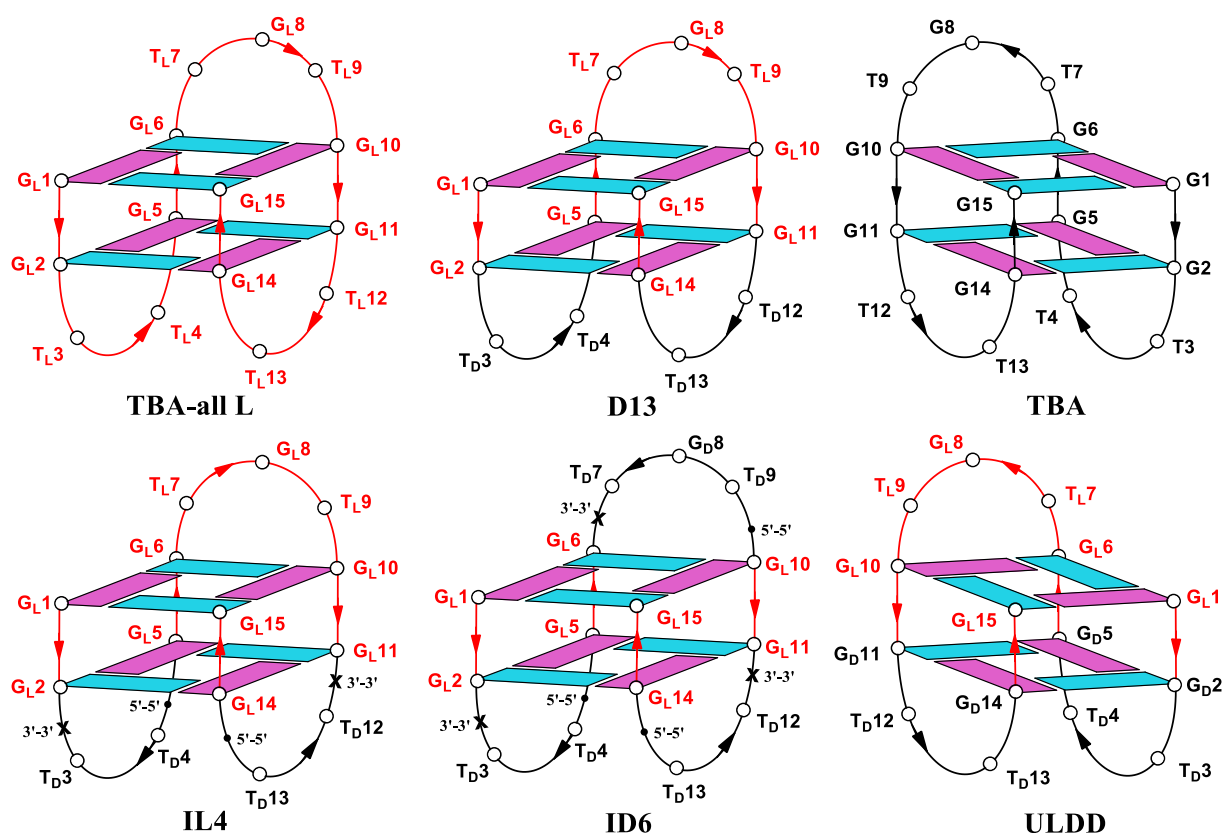
Fig. 1. Proposed G-quadruplex structures for the ODNs investigated (Table 1). *Anti* and *syn* guanosines are indicated in light blue and purple, respectively. The 3′–3′ and 5′–5′ inversion of polarity sites are indicated by a x and a dot, respectively. Arrows indicate the 5′–3′ orientation. D- and L-residues are labelled in black and red, respectively.

chair-like G-quadruplex structure very similar to that of the original **TBA**, except for the helix type [20]. Differently from **D13** and **TBA all-L**, ODNs **IL4**, **ID6** and **ULDD** have shown ^{1}H NMR spectra characterized by large and partially overlapped signals suggesting the presence of more than one conformation in equilibrium and, then, preventing us to carry out further detailed investigations. Nevertheless, also in these cases, the occurrence of signals in the diagnostic region has confirmed the presence of G-quadruplex structures that was already suggested by the CD profiles.

3.2. Biological activity

In order to evaluate the anticoagulant activity of the TBA analogues (Table 1), the modified sequences have been subjected to prothrombin time (PT) assay. This analysis has shown that none of the TBA

derivatives investigated is endowed with an anticoagulant activity, although high ODN concentrations have been used (Fig. 4).

The antiproliferative properties of the investigated ODNs (Table 1) have been tested on two different human cancerous cell lines, namely Calu-6 and HCT 116$^{p53 -/-}$. Two concentrations of ODNs, 10 μM and 50 μM, at different time points from 24 h to 144 h have been tested for their antiproliferative activities in Calu-6 and HCT 116$^{p53 -/-}$ cells, lung and colon cancer cell lines, respectively. Representative cell survival curves are given in Figs. 5 and 6. In Calu-6 cells, all ODNs have been found to have activity (Fig. 5). Among the tested ODNs, **ULDD** has the greatest effect on cell viability at both tested concentrations. Specifically, **ULDD** shows the 50% of its antiproliferative activity on tumor cells after lower incubation times (about 53 h and 52 h for concentrations 10 μM and 50 μM, respectively) than those observed for TBA (about 61 h and 55 h for concentrations 10 μM and 50 μM, respectively) (Table S1). The other ODNs have similar specificity, but they have
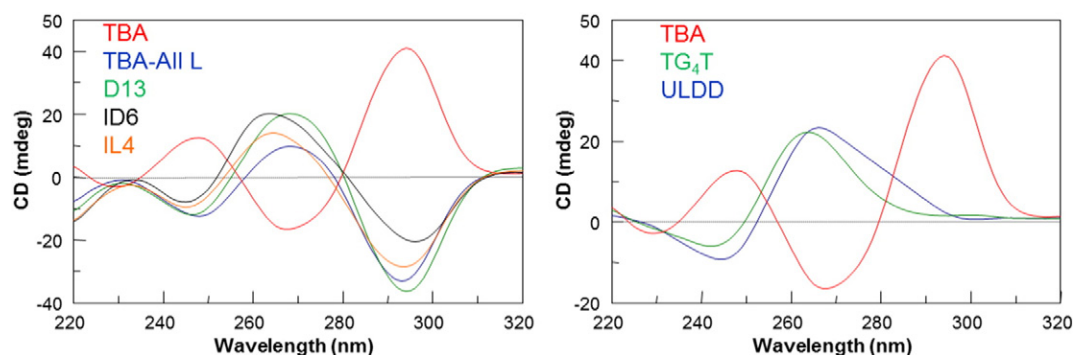

Fig. 2. CD spectra of the ODNs investigated (Table 1) (20 °C in a buffer solution 10 mM KH$_2$PO$_4$/K$_2$HPO$_4$, 70 mM KCl, pH = 7, ODN conc. = 1 × 10^{-4} M). The spectrum of the TG$_4$T parallel G-quadruplex has been shown as a reference.
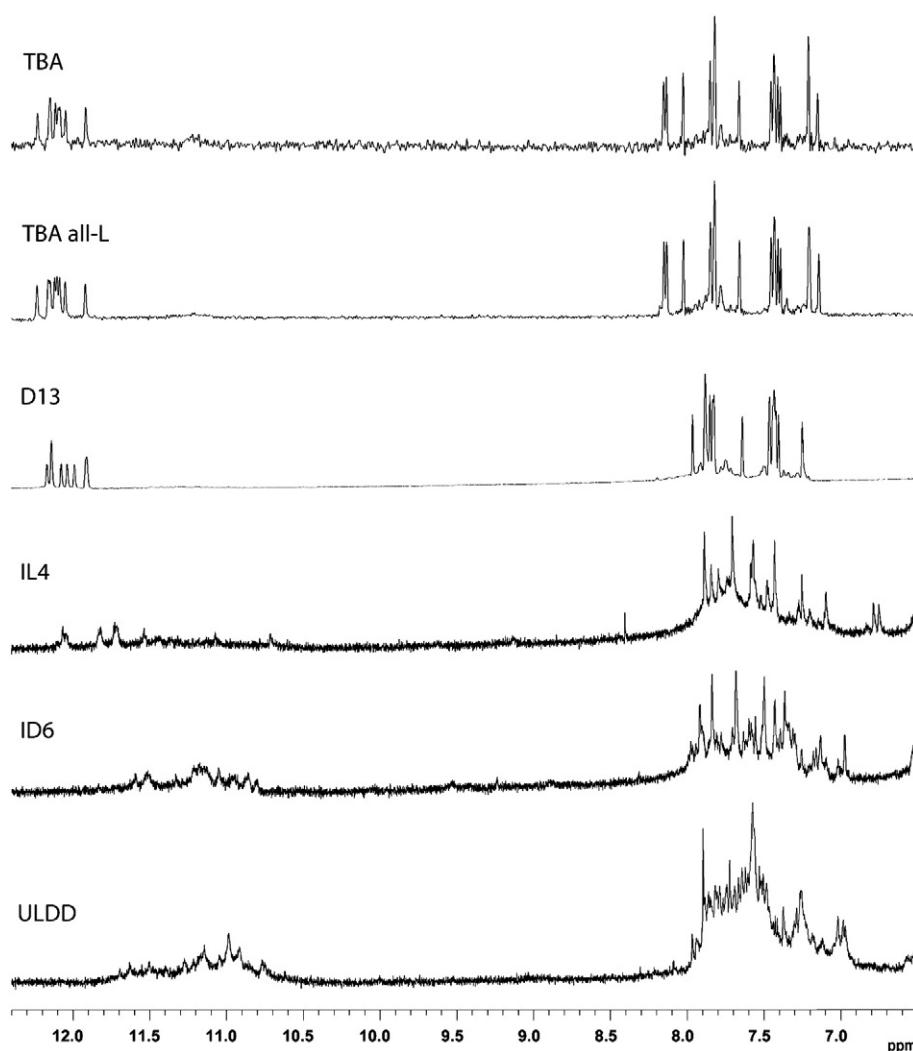
Fig. 3. ¹H NMR spectra of the ODNs investigated (Table 1). See Experimental section for details.

been less effective in inhibiting cell viability of cancer cells. However, all tested ODNs reduced the cell viability of Calu-6 cells from 10% to 1% after 144 h. We have observed **ID6**, **ULDD** and TBA active also in HCT 116$^{p53-/-}$ cell line in a time dependent manner (Fig. 6), while **TBA all-L**, **D13** and **IL4** have showed a different trend. In fact, for these
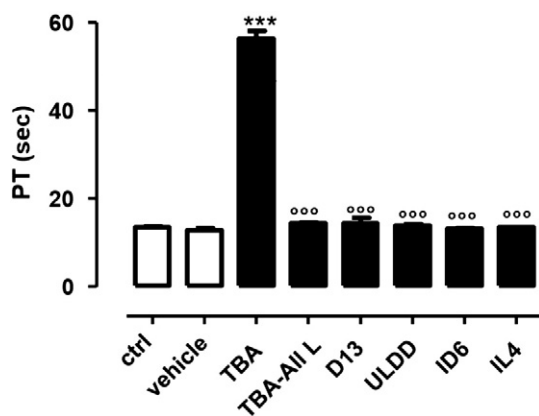
ODNs we have observed a decreased cytotoxicity after 96 h of incubation at 10 μM and for **DI3** and **IL4** also at 50 μM after 96 and 120 h of incubation, respectively. We hypothesize that the observed lower antiproliferative effect of these ODNs in HCT 116$^{p53-/-}$ cells could be a consequence of the activation of specific intracellular signalling pathways in response to treatment with these molecules able to inhibit their activity. In fact, several reports demonstrate that some chemical compounds exhibit specific cytotoxicity against a particular cancer cell type but not others. Furthermore, drug screening efforts have identified several compounds with cell type specificity [37,38].

Our analysis reveals that all tested ODNs exhibited a potent cytotoxicity in Calu-6 cells whereas the compounds **TBA all-L**, **D13** and **IL4** show different cytotoxicity in Calu-6 and HCT 116$^{p53-/-}$ suggesting that these two cell lines possess distinct survival signals that could lead to a different half-life of these ODNs. Future analysis of these compounds will have to be performed on additional human cancer cell lines to determine if this selectivity could conduct to the discovery of novel specific anti-lung cancer agents.

3.3. Nucleases stability assay

In order to test the resistance in biological environments, all TBA analogues were undergone to a degradation assay in fetal bovine serum and analyzed by gel electrophoresis (Fig. 7). Since the cell viability measured through the MTT assays has been tested up to

Fig. 4. PT values of the modified TBAs and their natural counterpart at 20 μM ODN concentration and incubation time of 15 min. See Experimental section for details. *** = $p < 0.001$ vs. vehicle, ° = $p < 0.05$, °° = $p < 0.01$, °°° = $p < 0.001$ vs. TBA (n = 3).
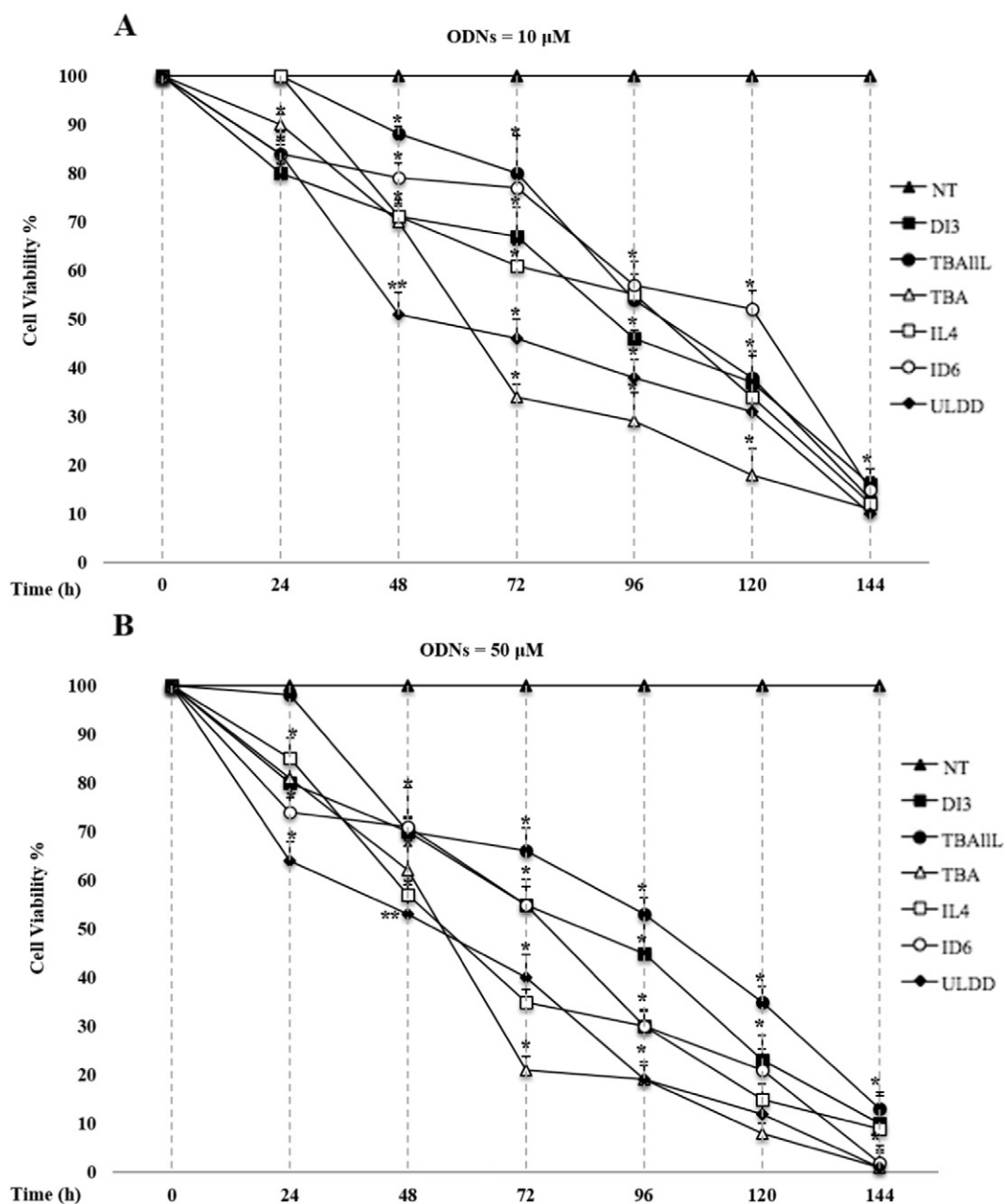
Fig. 5. Antiproliferative activity of ODNs on Calu 6 cell line. Cells were treated with two concentrations of ODNs, 10 μM (A) and 50 μM (B), from 24 to 144 h. The line NT (not treated) reports the cell viability in absence of ODNs. Cell viability was assayed 24, 48, 72, 96, 120 and 144 h after addition of ODNs using the MTT assay. Results are presented as percentage (mean ± SEM) (n = 3) of the control cells. *p < 0.05, **p < 0.01.

144 h, the resistance of ODNs in fetal bovine serum has been evaluated after the same time. As expected, ODNs mostly composed by L-residues have shown a slight (**IL4** and **D13**) or no detectable degradation (**TBA all-L**) in these conditions, while their natural counterpart TBA has been completely degraded. On the other hand, **ID6** has shown only a partial resistance, while **ULDD** has been almost completely degraded. Taking into consideration that both the 3′- and 5′-ends of all modified TBA derivatives show L-residues, it is improbable that the observed degradation could be due to the exonucleases. A plausible explanation is that, with a reaction time rather extended, the degradation could be induced by endonucleases. This assumption is corroborated by the stability trend observed in these conditions (**TBA all-L** > **IL4** > **D13** > **ID6** ≫ **ULDD**) that is quite in agreement with the amount of canonical 3′–5′ phosphodiester bonds present in the ODN sequences (0, 2, 2, 4 and 6 for ODNs **TBA all-L**, **IL4**, **D13**, **ID6** and **ULDD**, respectively).

4. Conclusions

Taking into account their structures and targets, the antiproliferative G-quadruplex aptamers (then potentially endowed with anticancer properties), appear as group rather heterogeneous of ligands. This datum is not particularly surprising considering the dependence of the cellular proliferation on several biological pathways, which implies a quite high number of potential targets. For example, a compelling amount of investigations strongly suggest that the target of the most studied antiproliferative G-quadruplex aptamer, namely the 26-mer AS1411, is the nucleolin, a multifunctional protein overexpressed in cytoplasm and on cell surface of many tumor types [39,40]. However, this frame is complicated by further data, among which are: 1) the recent finding that the cytotoxicity of guanine-based degradation products contributes to the antiproliferative activity of G-rich
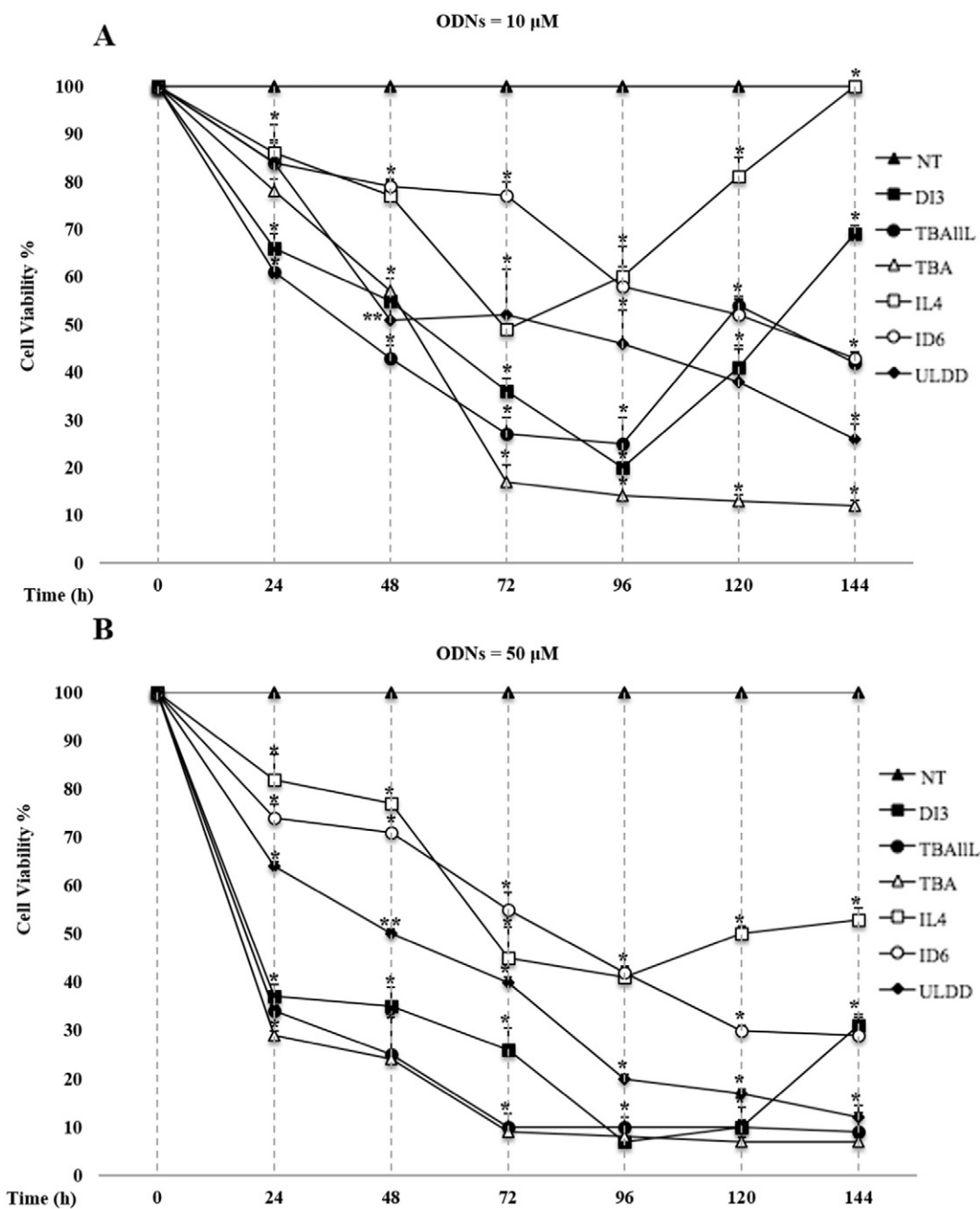
Fig. 6. Antiproliferative activity of ODNs on HCT 116$^{p53-/-}$ cell line. Cells were treated with two different concentrations of ODNs, 10 μM (A) and 50 μM (B), from 24 to 144 h. The line NT (not treated) reports the cell viability in absence of ODNs. Cell viability was assayed 24, 48, 72, 96, 120 and 144 h after addition of ODNs using the MTT assay. Results are presented as percentage (mean ± SEM) (n = 3) of the control cells. *p < 0.05, **p < 0.01.

oligonucleotides as AS1411 and other G-rich sequences [41] and 2) the extreme polymorphism of aptamer AS1411 [15]. On the other hand, the 16-mer aptamer T40214 (GGGC)$_4$ (and its analogues), forming a well-defined parallel G-quadruplex structure, is able to link the signal transducer and activator of transcription 3 protein (Stat3) [7,42], which is involved in a variety of cellular and biological processes including proliferation, differentiation, apoptosis, host defense, and transformation. Differently from these two aptamers, for which unique targets have been proposed, and according to literature data, the antiproliferative activity of TBA would depend on three factors: 1) the ability of TBA to interact with a protein thought to be nucleolin [10], 2) the involvement of thrombin, the main target of TBA, in promoting proliferation by interacting with the protease activated receptor-1 (PAR1) [43], and 3) similarly to other G-rich ODNs, the contribution of the guanine-based degradation products [41], particularly taking into account the

low resistance of TBA to nucleases [44]. Although the anticoagulant activity of TBA clearly represents a disadvantage in exploiting the antiproliferative property of this aptamer, a recent research has shown that suitable chemical sequence modifications can preserve its antiproliferative over anticoagulant activity [19]. Following a similar strategy, in this paper, we have investigated the properties of TBA analogues containing two modifications (Table 1), namely the presence of L-residues [20,36] and the introduction of inversion of polarity sites [21,45–47]. NMR and CD data suggest that all ODNs fold in G-quadruplex structures, although characterized by different helix types (right- or left-handed). Collected data are consistent with the occurring of "chair-like" G-quadruplex conformations resembling that of TBA, also in these cases. Importantly, none of the tested ODNs have shown anticoagulant activity (Fig. 4), thus suggesting that the TBA analogues are unable to interact with thrombin. However, MTT assays
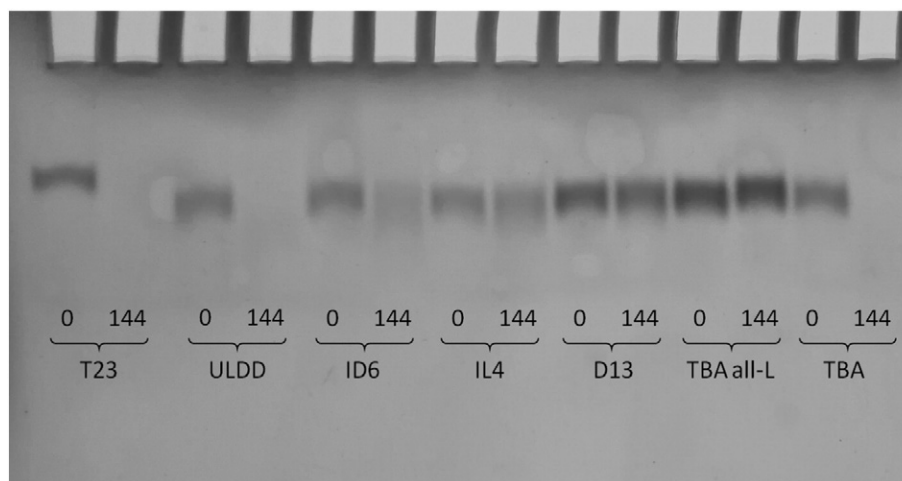
Fig. 7. Stability of the ODNs investigated in 10% fetal bovine serum (FBS), as monitored by non-denaturing PAGE. Time points 0 and 144 are in hours. ODN T23 has been used as positive control. See the Materials and methods section for experimental details.

concerning two types of cancer cells have indicated antiproliferative activities, in several cases, comparable with that of the natural TBA, depending on the cell type, sequence, time of treatment and ODN concentration. For example, the behavior of **TBA all-L** and TBA on HCT 116$^{p53-/-}$ cell line at 50 μm of ODN concentration is quite similar (Fig. 6). On the other hand, for time of treatment of 144 h, the antiproliferative activity on Calu 6 cell line has resulted comparable to TBA for most of the tested ODNs (Fig. 5). NMR and CD data have clearly indicated that, among the ODNs investigated, **TBA all-L** and **D13** adopt well-defined "chair-like" left-handed G-quadruplex structures [20]. However, contrarily to TBA, their antiproliferative activities cannot be ascribed neither to the interaction with the thrombin (since they do not show an anticoagulant activity) neither to the guanine-based products derived from their degradation (since they are quite resistant to nucleases and their potential degradation products would be mostly L-residues). On the other hand, although it cannot be ruled out definitively, it is quite improbable that the target is nucleolin also for **TBA all-L** and **D13**, since they adopt left-handed G-quadruplex structures, which are the mirror image of the TBA one. Interestingly, a possible relationship between the left-handed G-quadruplex structure adopted by an AS1411 related ODN [16] and that one formed by **TBA all-L** and **D13** could be hypothesized. These observations suggest that the antiproliferative activity of **TBA all-L** and **D13** could depend on biological pathways and targets different from those taken into account up to now. Biochemical experiments in this frame are underway in our laboratories. Similar considerations could be applied also for **IL4** and **ID6**, similarly showing noteworthy antiproliferative activities (particularly against Calu-6 cell line), although, in these cases, their partial degradability does not allow to rule out completely the contribution of the guanine-based degradation products. Taking into consideration the low biological resistance of **ULDD**, which among the other ODNs has shown the most interesting results, the contribution of the guanine-based degradation products to the antiproliferative activity could be even higher than the other TBA derivatives. In the case of **ULDD**, a right-handed G-quadruplex structure has been suggested, although details concerning its conformation are lacking. In order to stabilize its G-quadruplex structure and increase the biological resistance, we have planned the preparation of derivatives containing site-specific replacement of guanosines supposed to adopt *anti* and *syn* glycosidic conformations, with modified nucleotides known to promote them (as for example, LNA [48] and 8-methyl-2′-deoxyguanosine [49,50] residues, respectively), with the aim to investigate the involvement of different biological pathways and targets in the observed antiproliferative activity.

Transparency document

The Transparency document associated with this article can be found, in online version.

Appendix A. Supplementary data

Supplementary data to this article can be found online at http://dx.doi.org/10.1016/j.bbagen.2016.09.019.

References

[1] For a recent general review see:. F. Radom, P.M. Jurek, M.P. Mazurek, J. Otlewski, F. Jeleń, Aptamers: molecules of great potential, Biotechnol. Adv. 31 (2013) 1260–1274.
[2] Y.X. Wu, Y.J. Kwon, Aptamers: the "evolution" of SELEX, Methods (2016), http://dx.doi.org/10.1016/j.ymeth.2016.04.020.
[3] A. Varizhuk, N. Ilyinsky, I. Smirnov, G. Pozmogova, G4 aptamers: trends in structural design, Mini Rev. Med. Chem. (2016), http://dx.doi.org/10.2174/1389557516666160321114715.
[4] W.O. Tucker, K.T. Shum, J.A. Tanner, G-quadruplex DNA aptamers and their ligands: structure, function and application, Curr. Pharm. Des. 18 (2012) 2014–2026.
[5] J.E. Rosenberg, R.M. Bambury, E.M. Van Allen, H.A. Drabkin, P.N. Lara Jr., A.L. Harzstark, N. Wagle, R.A. Figlin, G.W. Smith, L.A. Garraway, T. Choueiri, F. Erlandsson, D.A. Laber, A phase II trial of AS1411 (a novel nucleolin-targeted DNA aptamer) in metastatic renal cell carcinoma, Investig. New Drugs 32 (2014) 178–187.
[6] M.T. Malik, M.G. O'Toole, L.K. Casson, S.D. Thomas, G.T. Bardi, E.M. Reyes-Reyes, C.K. Ng, K.A. Kang, P.J. Bates, AS1411-conjugated gold nanospheres and their potential for breast cancer therapy, Oncotarget 26 (2015) 22270–22281.
[7] N. Jing, Y. Li, W. Xiong, W. Sha, L. Jing, D.J. Tweardy, G-quartet oligonucleotides: a new class of signal transducer and activator of transcription 3 inhibitors that suppresses growth of prostate and breast tumors through induction of apoptosis, Cancer Res. 64 (2004) 6603–6609.
[8] J. Hu, Z. Zhao, Q. Liu, M. Ye, B. Hu, J. Wang, W. Tan, Study of the function of G-rich aptamers selected for lung adenocarcinoma, Chem. Asian J. 10 (2015) 1519–1525.
[9] E.W. Choi, L.V. Nayak, P.J. Bates, Cancer-selective antiproliferative activity is a general property of some G-rich oligodeoxynucleotides, Nucleic Acids Res. 38 (2010) 1623–1635.
[10] V. Đapić, V. Abdomerovič, R. Marrington, J. Peberdy, A. Rodger, J.O. Trent, P.J. Bates, Biophysical and biological properties of quadruplex oligodeoxyribonucleotides, Nucleic Acids Res. 31 (2003) 2097–2107.
[11] A.C. Girvan, Y. Teng, L.K. Casson, S.D. Thomas, S. Jüliger, M.W. Ball, J.B. Klein, W.M. Pierce Jr., S.S. Barve, P.J. Bates, AGRO100 inhibits activation of nuclear factor kappa B (NF-kappaB) by forming a complex with NF-kappaB essential modulator (NEMO) and nucleolin, Mol. Cancer Ther. 5 (2006) 1790–1799.

[12] Y. Teng, A.C. Girvan, L.K. Casson, W.M. Pierce Jr., M. Qian, S.D. Thomas, P.J. Bates, AS1411 alters the localization of a complex containing protein arginine methyltransferase 5 and nucleolin, Cancer Res. 67 (2007) 10491–10500.

[13] P.J. Bates, D.A. Laber, D.M. Miller, S.D. Thomas, J.O. Trent., Discovery and development of the G-rich oligonucleotide AS1411 as a novel treatment for cancer, Exp. Mol. Pathol. 86 (2009) 151–164.

[14] P.J. Bates, J.B. Kahlon, S.D. Thomas, J.O. Trent, D.M. Miller, Antiproliferative activity of G-rich oligonucleotides correlates with protein binding, J. Biol. Chem. 274 (1999) 26369–26377.

[15] M.M. Dailey, M. Clarke Miller, P.J. Bates, A.N. Lane, J.O. Trent, Resolution and characterization of the structural polymorphism of a single quadruplex-forming sequence, Nucleic Acids Res. 38 (2010) 4877–4888.

[16] W.J. Chung, B. Heddi, E. Schmitt, K.W. Lim, Y. Mechulam, A.T. Phan, Structure of a left-handed DNA G-quadruplex, Proc. Natl. Acad. Sci. U. S. A. 112 (2015) 2729–2733.

[17] R.F. Macaya, P. Schultze, F.W. Smith, J.A. Roe, J. Feigon, Thrombin-binding DNA aptamer forms a unimolecular quadruplex structure in solution, Proc. Natl. Acad. Sci. U. S. A. 90 (1993) 3745–3749.

[18] J.A. Kelly, J. Feigon, T.O. Yeates, Reconciliation of the X-ray and NMR structures of the thrombin-binding aptamer d(GGTTGGTGTGGTTGG), J. Mol. Biol. 256 (1996) 417–422.

[19] M. Scuotto, E. Rivieccio, A. Varone, D. Corda, M. Bucci, V. Vellecco, G. Cirino, A. Virgilio, V. Esposito, A. Galeone, N. Borbone, M. Varra, L. Mayol, Site specific replacements of a single loop nucleoside with a dibenzyl linker may switch the activity of TBA from anticoagulant to antiproliferative, Nucleic Acids Res. 43 (2015) 7702–7716.

[20] A. Virgilio, M. Varra, M. Scuotto, A. Capuozzo, C. Irace, L. Mayol, V. Esposito, A. Galeone, Expanding the potential of G-quadruplex structures: formation of a heterochiral TBA analogue, Chembiochem 155 (2014) 652–655.

[21] A. Virgilio, L. Mayol, M. Varra, A. Galeone, V. Esposito, Unusual chair-like G-quadruplex structures: heterochiral TBA analogues containing inversion of polarity sites, J. Chem. (2015), 473051.

[22] C. Dalvit, Efficient multiple-solvent suppression for the study of the interactions of organic solvents with biomolecules, J. Biomol. NMR 11 (1998) 437–444.

[23] F. Bunz, A. Dutriaux, C. Lengauer, T. Waldman, S. Zhou, J.P. Brown, J.M. Sedivy, K.W. Kinzler, B. Vogelstein, Requirement for p53 and p21 to sustain G2 arrest after DNA damage, Science 282 (1998) 1497–1501.

[24] A. Russo, V. Pagliara, F. Albano, D. Esposito, V. Sagar, F. Loreni, C. Irace, R. Santamaria, G. Russo, Regulatory role of rpL3 in cell response to nucleolar stress induced by Act D in tumor cells lacking functional p53, Cell Cycle 15 (2016) 41–51.

[25] D. Esposito, E. Crescenzi, V. Sagar, F. Loreni, A. Russo, G. Russo, Human rpL3 plays a crucial role in cell response to nucleolar stress induced by 5-FU and L-OHP, Oncotarget 5 (2014) 11737–11751.

[26] S. Maiolino, A. Russo, V. Pagliara, C. Conte, F. Ungaro, G. Russo, F. Quaglia, Biodegradable nanoparticles sequentially decorated with polyethyleneimine and hyaluronan for the targeted delivery of docetaxel to airway cancer cells, J. Nanobiotechnol. 13 (2015) 29.

[27] D. De Filippis, A. Russo, D. De Stefano, M. Cipriano, D. Esposito, G. Grassia, R. Carnuccio, G. Russo, T. Iuvone, Palmitoylethanolamide inhibits rMCP-5 expression by regulating MITF activation in rat chronic granulomatous inflammation, Eur. J. Pharmacol. 15 (2014) 64–69.

[28] K. Padmanabhan, A. Tulinsky, An ambiguous structure of a DNA 15-mer thrombin complex, Acta Crystallogr. Sect. D Biol. Crystallogr. D52 (1996) 272–282.

[29] A. Avino, C. Fabrega, M. Tintore, R. Eritja, Thrombin binding aptamer, more than a simple aptamer: chemically modified derivatives and biomedical applications, Curr. Pharm. Des. 18 (2012) 2036–2047.

[30] I. Russo Krauss, A. Merlino, C. Giancola, A. Randazzo, L. Mazzarella, F. Sica, Thrombin-aptamer recognition: a revealed ambiguity, Nucleic Acids Res. 39 (2011) 7858–7867.

[31] M. Vorlíčková, I. Kejnovská, J. Sagi, D. Renčiuk, K. Bednářová, J. Motlová, J. Kypr, Circular dichroism and guanine quadruplexes, Methods 57 (2012) 64–75.

[32] I. Russo Krauss, A. Merlino, A. Randazzo, E. Novellino, L. Mazzarella, F. Sica, High resolution structures of two complexes between thrombin and thrombin-binding aptamer shed light on the role of cations in the aptamer inhibitory activity, Nucleic Acids Res. 40 (2012) 8119–8128.

[33] R. Reshetnikov, A. Golovin, A. Kopylov, J. Šponer, Structural dynamics of thrombin binding DNA aptamer d(GGTTGGTGTGGTTGG) quadruplex DNA studied by large-scale explicit solvent simulations, J. Chem. Theory Comput. 6 (2010) 3003–3014.

[34] S. Nagatoishi, N. Sugimoto, Interaction of water with the G-quadruplex loop contributes to the binding energy of G-quadruplex to protein, Mol. BioSyst. 8 (2012) 2766–2770.

[35] S. Masiero, R. Trotta, S. Pieraccini, S. De Tito, R. Perone, A. Randazzo, G.P. Spada, A non-empirical chromophoric interpretation of CD spectra of DNA G-quadruplex structures, Org. Biomol. Chem. 8 (2010) 2683–2692.

[36] A. Virgilio, V. Esposito, G. Citarella, A. Mangoni, L. Mayol, A. Galeone, Unprecedented right- and left-handed quadruplex structures formed by heterochiral oligodeoxyribonucleotides, Biochimie 93 (2011) 1193–1196.

[37] K.W. Yip, X. Mao, P.Y. Au, D.W. Hedley, S. Chow, S. Dalili, J.D. Mocanu, C. Bastianutto, A. Schimmer, F.F. Liu, Benzethonium chloride: a novel anticancer agent identified by using a cell-based small-molecule screen, Clin. Cancer Res. 12 (2006) 5557–5569.

[38] H. Kashida, H. Ito, T. Fujii, T. Hayashi, H. Asanuma, Positively charged base surrogate for highly stable "base pairing" through electrostatic and stacking interactions, J. Am. Chem. Soc. 131 (2009) 9928–9930.

[39] S. Christian, J. Pilch, M.E. Akerman, K. Porkka, P. Laakkonen, E. Ruoslahti, Nucleolin expressed at the cell surface is a marker of endothelial cells in angiogenic blood vessels, J. Cell Biol. 163 (2003) 871–878.

[40] H. Ginisty, H. Sicard, B. Roger, P. Bouvet, Structure and functions of nucleolin, J. Cell Sci. 112 (1999) 761–772.

[41] N. Zhang, T. Bing, X. Liu, C. Qi, L. Shen, L. Wanga, D. Shangguan, Cytotoxicity of guanine-based degradation products contributes to the antiproliferative activity of guanine-rich oligonucleotides, Chem. Sci. 6 (2015) 3831–3838.

[42] P. Weerasinghe, Y. Li, Y. Guan, R. Zhang, D.J. Tweardy, N. Jing, T40214/PEI complex: a potent therapeutics for prostate cancer that targets STAT3 signaling, Prostate 68 (2008) 1430–1442.

[43] S. Zhou, W. Xiao, X. Pan, M. Zhu, Z. Yang, F. Zhang, C. Zheng, Thrombin promotes proliferation of human lung fibroblasts via protease activated receptor-1-dependent and NF-kB-independent pathways, Cell Biol. Int. 38 (2014) 747–756.

[44] C. Geng Peng, M.J. Damha, G-quadruplex induced stabilization by 2′-deoxy-2′-fluoro-D-arabinonucleic acids (2′F-ANA), Nucleic Acids Res. 35 (2007) 4977–4988.

[45] V. Esposito, A. Virgilio, A. Pepe, G. Oliviero, L. Mayol, A. Galeone, Effects of the introduction of inversion of polarity sites in the quadruplex forming oligonucleotide TGGGT, Bioorg. Med. Chem. 17 (2009) 1997–2001.

[46] P. Sket, A. Virgilio, V. Esposito, A. Galeone, J. Plavec, Strand directionality affects cation binding and movement within tetramolecular G-quadruplexes, Nucleic Acids Res. 40 (2012) 11047–11057.

[47] A. Virgilio, V. Esposito, R. Filosa, L. Mayol, A. Galeone, The introduction of inversion of polarity sites in DNA G-quadruplex structures: effects and perspectives, Mini Rev. Med. Chem. 16 (2016) 509–523.

[48] A. Randazzo, V. Esposito, O. Ohlenschläger, R. Ramachandran, L. Mayol, NMR solution structure of a parallel LNA quadruplex, Nucleic Acids Res. 32 (2004) 3083–3092.

[49] P.L. Thao Tran, A. Virgilio, V. Esposito, G. Citarella, J.-L. Mergny, A. Galeone, Effects of 8-methylguanine on structure, stability and kinetics of formation of tetramolecular quadruplexes, Biochimie 93 (2011) 399–408.

[50] A. Virgilio, V. Esposito, G. Citarella, A. Pepe, L. Mayol, A. Galeone, The insertion of two 8-methyl-2′-deoxyguanosine residues in tetramolecular quadruplex structures: trying to orientate the strands, Nucleic Acids Res. 40 (2012) 461–475.